Supporting Information

Ultrafast Approach for the Syntheses of Defective Nanosized Lanthanide Perovskites for Catalytic Toluene Oxidation

Xiaole Weng[a], Wang Long Wang[a], Qingjie Meng[a] and Zhongbiao Wu*[a]

[a] Key Laboratory of Environment Remediation and Ecological Health, Ministry of Education, College of Environmental and Resource Sciences, Zhejiang University, Zhejiang Provincial Engineering Research Center of Industrial Boiler & Furnace Flue Gas Pollution Control, 388 Yuhangtang Road, Hangzhou, 310058, P. R. China.

Corresponding author: Dr. Zhongbiao Wu, Fax/Tel: 0086571 8795308; E-mail: zbwu@zju.edu.cn.

1. Catalyst syntheses

sc-H_2O route: In a typical synthesis (see **Fig. S1**), metal nitrate solution (with or without H_2O_2) and NaOH were separately pumped into the reactor by using HPLC pumps at a range of flow rates including 6 and 7.5 mL.min^{-1}. The two streams were mixed in a stainless steel Swagelok^{TM} 1/8" Tee" piece at room temperature, which was then carried to meet a stream of deionized water that was fed by another HPLC pumps at a certain flow rates (e.g. 25 and 30 mL.min^{-1}), heated beyond the supercritical temperature (at 374 ºC) by using an electric furnace and then transported through a stainless steel Swagelok^{TM} 1/16" tube into a confined jet mixer (i.e. reactor, a Swagelok^{TM} 1/4" cross[1]). An adjustable length band heater set to 550 ºC was added to reactor to maintain the reaction temperature. By altering the band heater length and flow velocity, the residence time can be tuned in a wide range. The precipitates formed in the confined jet mixer were cooled down to room temperature, passed through a 7 μm filter to remove large aggregates and then collected from the exit of

back-pressure regulator (that was used to maintain the system pressure at ca. 23.1 MPa). Solids were collected by centrifuging the slurry (5000 rpm, 5min) and then freeze-dried to obtain products as black colored fluffy powder. The advantage of jet mixer is that it enable the precursors to encounter with a high-speed jet of supercritical water, thus leading to a rapid and momentum-driven mixing for hybrid oxides. Another advantage is that such mixing route will maintain a high temperature for the reactor.

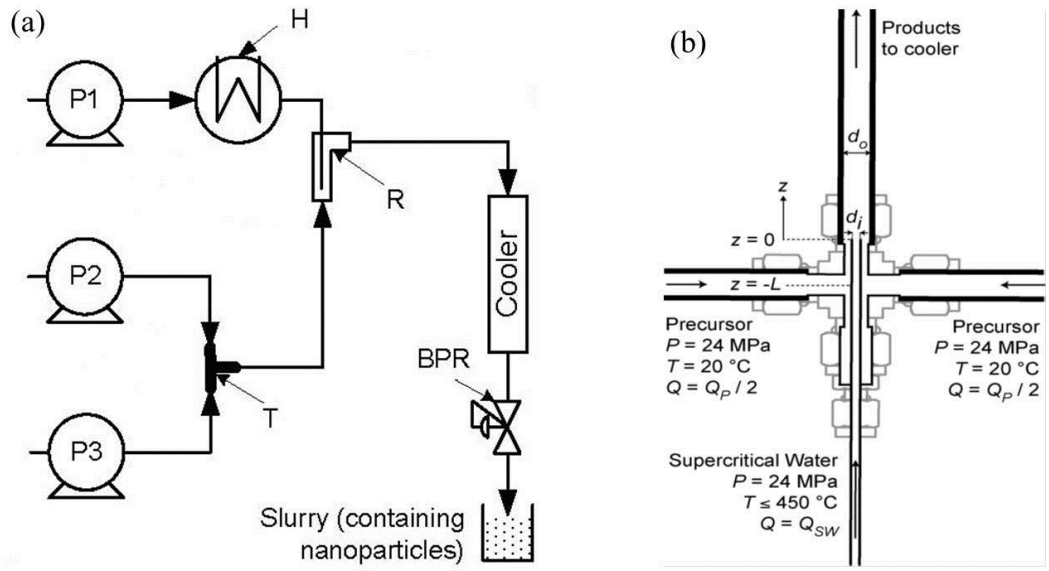

Fig. S1 (a) Schematic representation of the three-pump (P1–P3) continuous hydrothermal flow synthesis system that was used to prepare nanoparticles catalysts. Key: P = pump, BPR = back-pressure regulator, R = reactor, H = heater, T = T junction; (b) Schematic diagram of the confined jet reactor [Gruar, R. I.; Tighe, C. J.; Darr, J. A. Industrial & Engineering Chemistry Research 2013, 52 (15), 5270-5281].

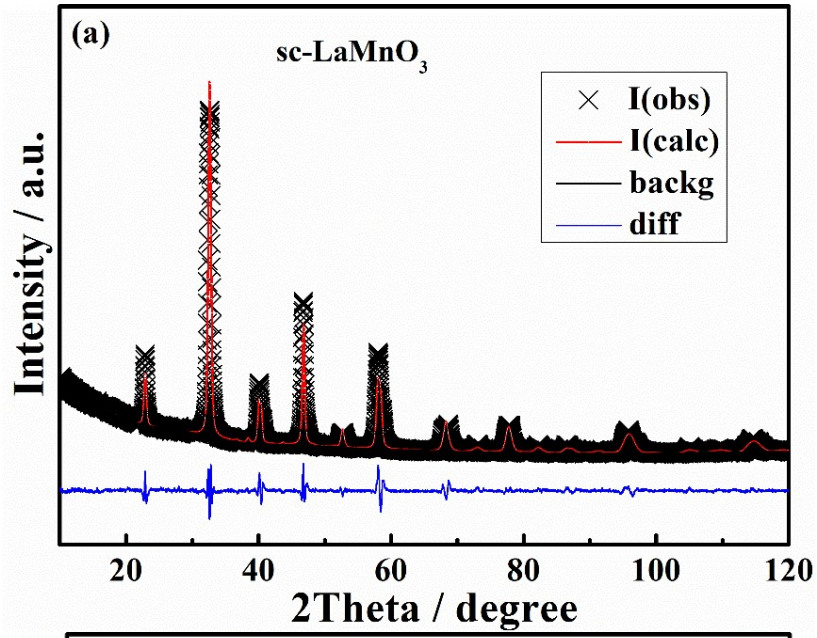
(a)
sc-LaMnO3
I(obs)
I(calc)
backg
diff
Intensity / a.u.
20
40
60
80
100
120
2Theta / degree

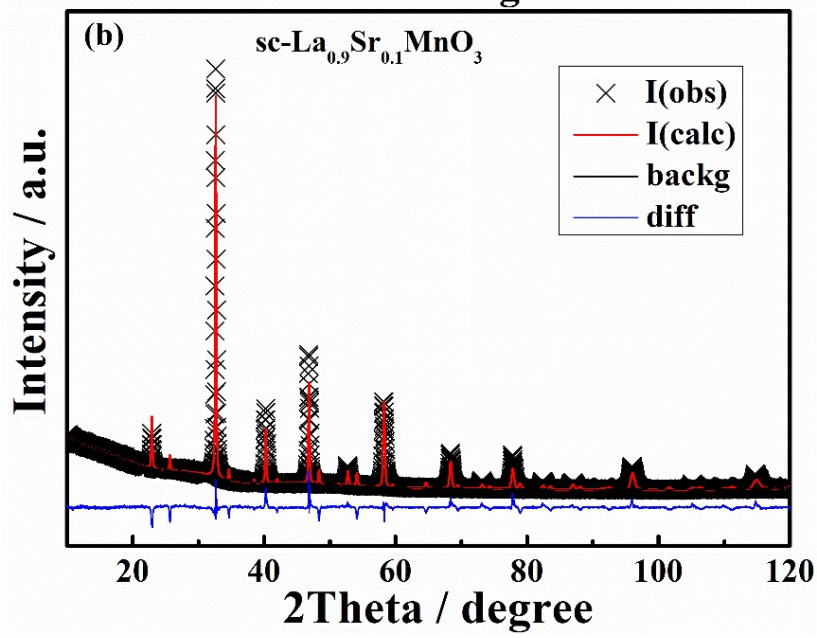
(b)
sc-La0.9Sr0.1MnO3
I(obs)
I(calc)
backg
diff
Intensity / a.u.
20
40
60
80
100
120
2Theta / degree

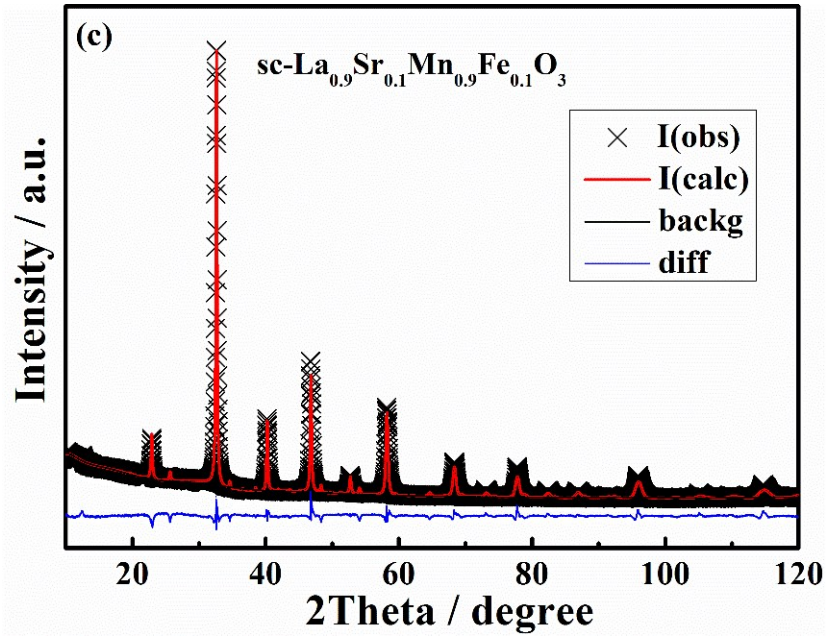

Fig. S2 Rietveld refinement data of (a) sc-$LaMnO_3$,(b) sc-$La_{0.9}Sr_{0.1}MnO_3$ and (c) sc-$La_{0.9}Sr_{0.1}Mn_{0.9}Fe_{0.1}O_3$ catalysts.

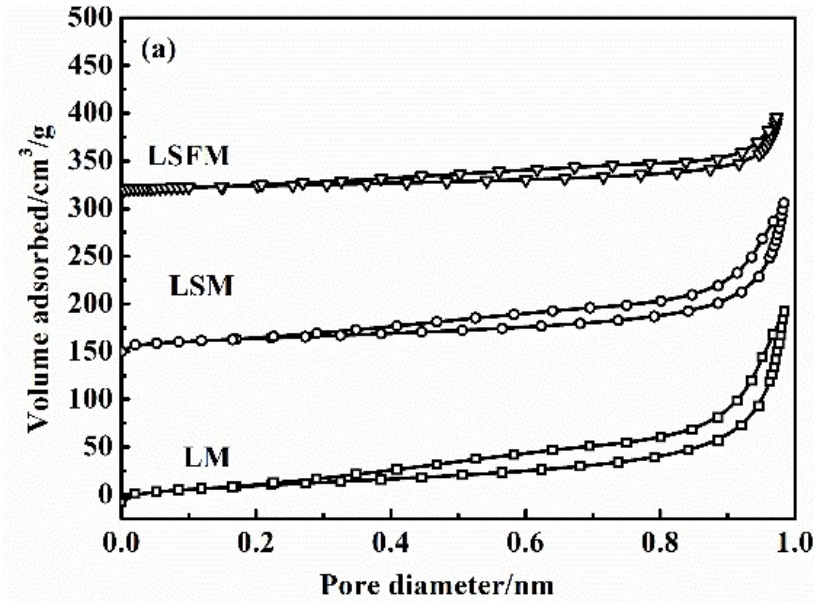

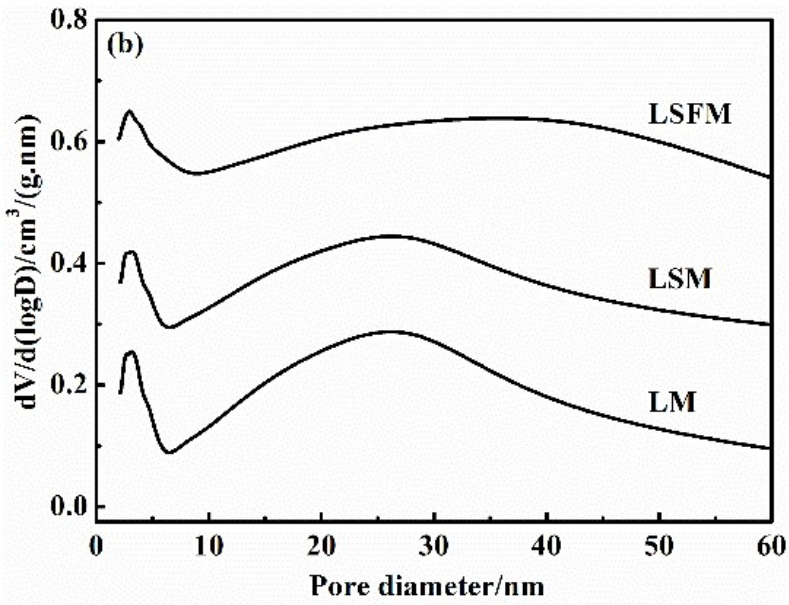

Fig. S3 (a) Nitrogen adsorption–desorption isotherms and (b) pore-size distributions of $LaMnO_3$, sc-$La_{0.9}Sr_{0.1}MnO_3$ and sc-$La_{0.9}Sr_{0.1}Mn_{0.9}Fe_{0.1}O_3$ catalysts.

Table. S1 BET surface areas, pore volume, average pore size of each catalyst.

catalyst	Surface area / m^2/g	Pore volume / cm^3/g	Average pore size / nm
sc-$LaMnO_3$	67.86	0.327	11.58
sc-$La_{0.9}Sr_{0.1}MnO_3$	52.69	0.254	13.83
sc-$La_{0.9}Sr_{0.1}Mn_{0.9}Fe_{0.1}O_3$	28.46	0.123	17.22

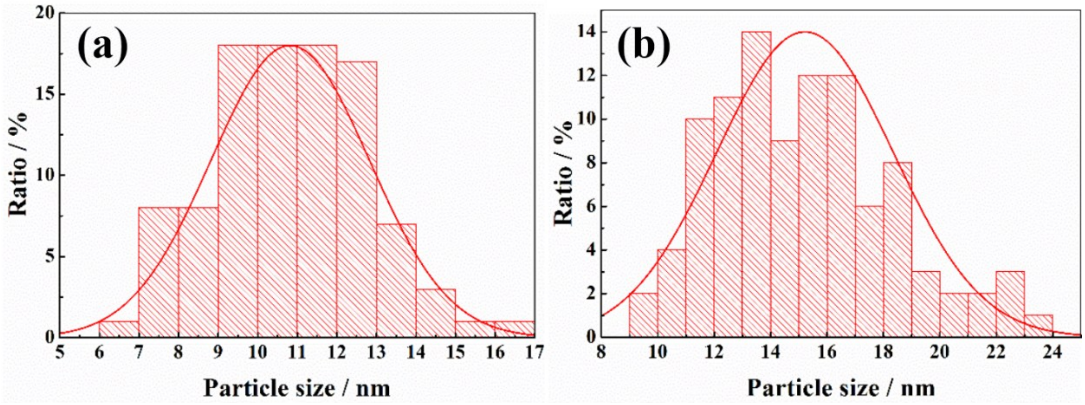

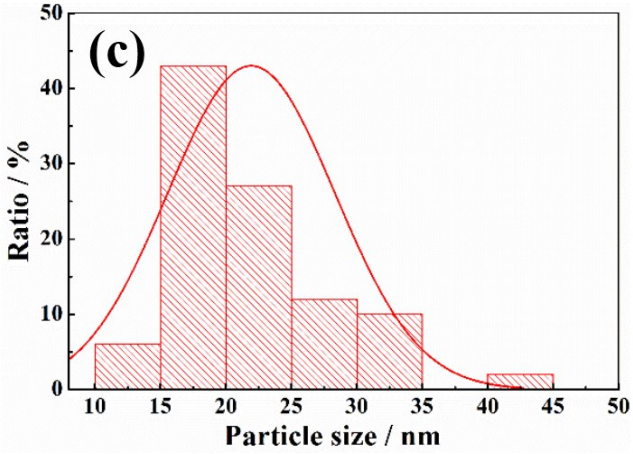

Fig. S4 Particle size distribution of (a) sc-$LaMnO_3$, (b) sc-$La_{0.9}Sr_{0.1}MnO_3$ and (c) sc-$La_{0.9}Sr_{0.1}Mn_{0.9}Fe_{0.1}O_3$ catalysts.

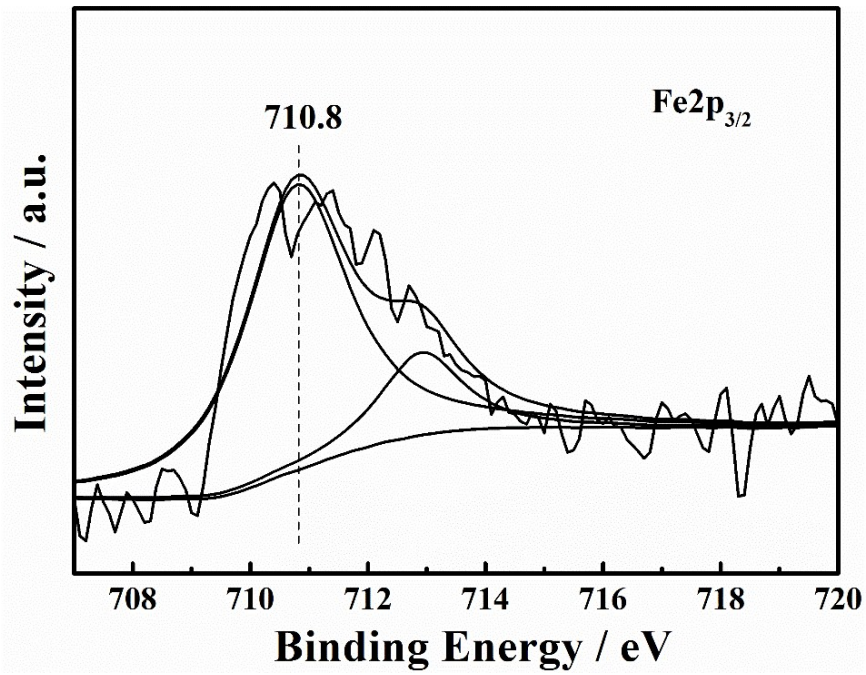

Fig. S5 $Fe2p_{3/2}$ spectra of sc-$La_{0.9}Sr_{0.1}Mn_{0.9}Fe_{0.1}O_3$ catalyst.

Table. S2 Summary of literature data on catalytic oxidation of toluene over the noble metal catalysts under a similar condition.

catalysts	Toluene concentration / ppm	GHSV / h^{-1} or $mL.g^{-1}.h^{-1}$	T_{90} /	Ref
0.5 wt.% Pd/C	1000	30000	361	[2]
1 wt.% Pt/CeO_2	1000	40000	225	[3]

1 wt.% Pt/Al_2O_3	600	60000	235	[4]
0.71wt.% Au/Fe_2O_3	1000	20000	250	[5]

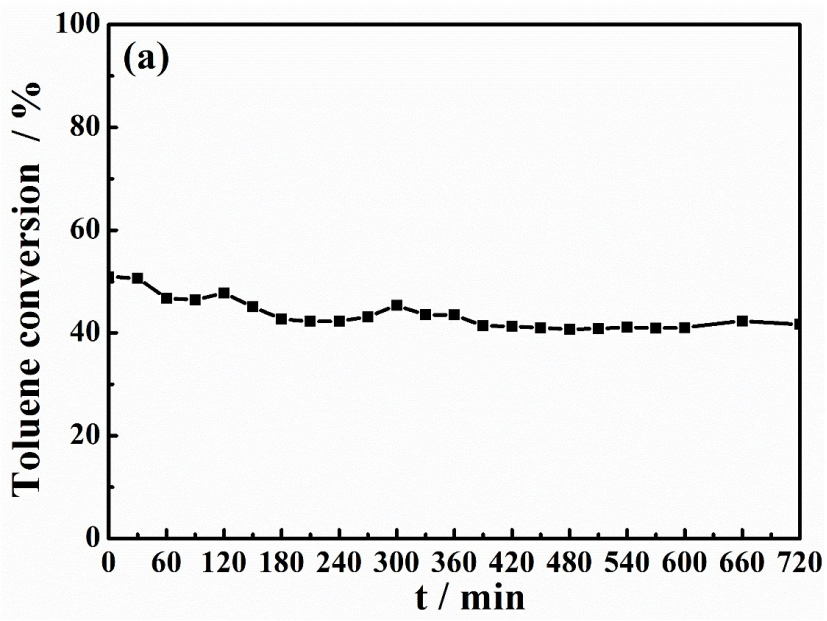

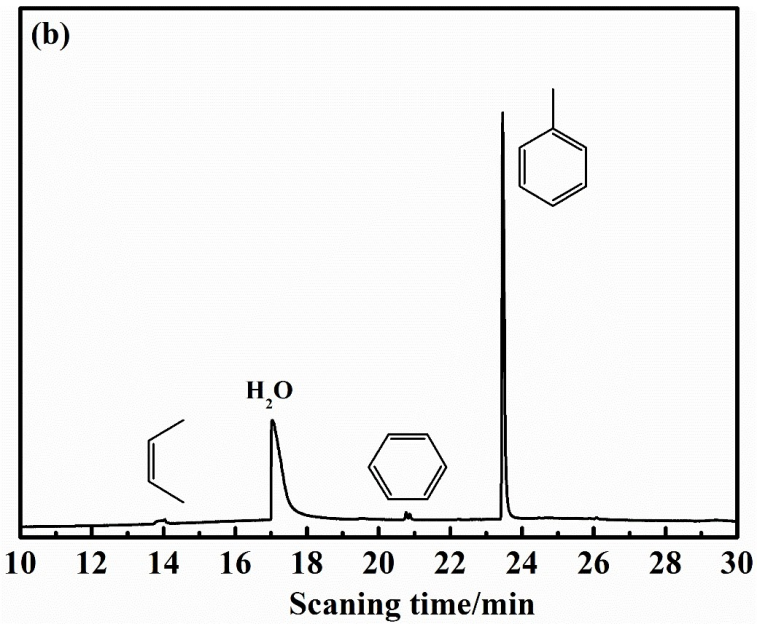

Fig. S6 (a) the time dependence curves of toluene conversion over sc-$La_{0.9}Sr_{0.1}Mn_{0.9}Fe_{0.1}O_3$ catalyst and **(b)** GC-MS analyses of the sc-$La_{0.9}Sr_{0.1}Mn_{0.9}Fe_{0.1}O_3$ after stability test.

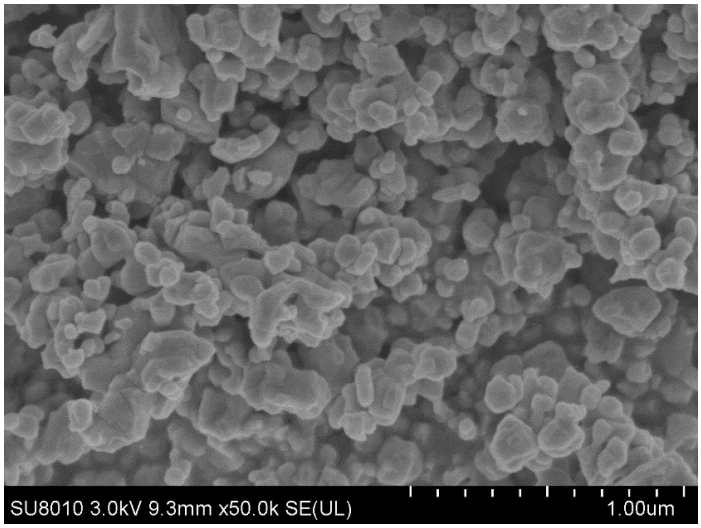

Fig. S7 SEM image of cr-$LaMnO_3$ sample.

Reference

1. R. I. Gruar, C. J. Tighe and J. A. Darr, *Ind. Eng. Chem. Res.*, 2013, **52**, 5270-5281.
2. S. Morales-Torres, F. J. Maldonado-Hódar, A. F. Pérez-Cadenas and F. Carrasco-Marín, *J. Hazard. Mater.*, 2010, **183**, 814-822.
3. Z. Abdelouahab-Reddam, R. E. Mail, F. Coloma and A. Sepúlveda-Escribano, *Appl. Catal., A*, 2015, **494**, 87-94.
4. A. M. Carrillo and J. G. Carriazo, *Appl. Catal., B*, 2015, **164**, 443-452.
5. W. Han, J. Deng, S. Xie, H. Yang, H. Dai and C. T. Au, *Ind. Eng. Chem. Res.*, 2014, **53**, 3486-3494.